PROBABILISTIC PREDICTION OF SEVERITY OF LIQUEFACTION SURFACE MANIFESTATION USING GEOTECHNICAL AND GEOSPATIAL MODELS

Brett W. Maurer[1], Sjoerd van Ballegooy[2], and Brendon A. Bradley[3]

[1] Dept. of Civil and Environmental Engineering, University of Washington, USA

[2] Tonkin + Taylor Ltd., Auckland, New Zealand

[3] Dept. of Civil and Natural Resources Engineering, University of Canterbury, New Zealand

ABSTRACT

The severity of liquefaction manifested at the ground surface is a pragmatic proxy of damage potential for various infrastructure assets, making it particularly useful for hazard mapping, land-use planning, and preliminary site-assessment. Towards this end, the recent Canterbury, New Zealand, earthquakes, in conjunction with others, have resulted in liquefaction case-history data of unprecedented quantity and quality, presenting a unique opportunity to develop fragility-functions for liquefaction-induced ground failure. Accordingly, this study analyzes nearly 10,000 liquefaction case studies from 23 earthquakes to develop functions that express the probability of exceeding specific severities of liquefaction surface-manifestation as a function of five different liquefaction damage measures (*LDMs*), of which three are based on geotechnical data and two are based on freely available geospatial data. The proposed functions have the same functional form, such that end-users can easily select the model coefficients for the particular damage state and *LDM* of their choosing. It should be noted that these functions are not to be used to predict lateral spreading, which requires *LDMs* other than those assessed herein. Lastly, the proposed functions are preliminary and subject to further development. In this regard, several thrusts of ongoing investigation are mentioned.

DATA

This study analyzes **9,908 liquefaction case histories** from **23 earthquakes** (Table 1). However, because the majority of these cases were compiled from three events during the 2010-2016 Canterbury Earthquake Sequence (CES), results are separately presented for these and the other 20 earthquakes, henceforth respectively referred to as the "CES dataset" and "global dataset." Components of the CES dataset[1] are highlighted in Figure 1.

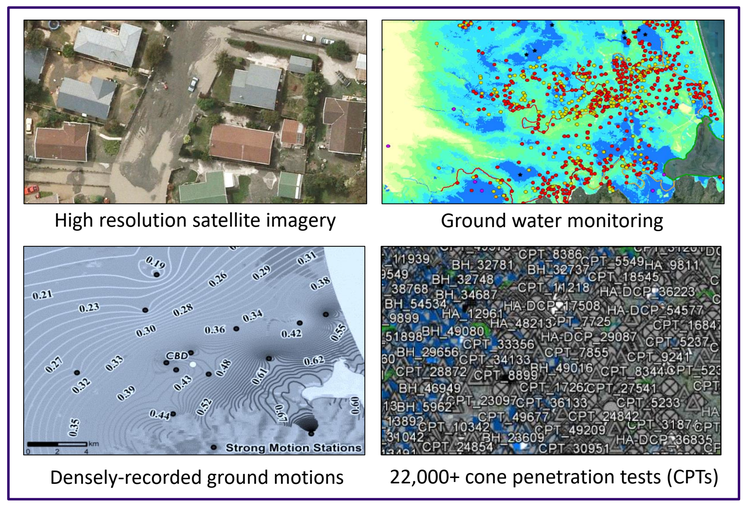

Figure 1. Select components of the CES dataset

Table 1. Summary of Liquefaction Case Studies Analyzed

Year	Earthquake	Country	M_w	# Cases
1964	Niigata	Japan	7.60	3
1971	San Fernando	USA	6.60	2
1975	Haicheng	China	7.00	2
1976	Tangshan	China	7.60	10
1979	Imperial Valley	USA	6.53	5
1980	Victora (Mexicali)	Mexico	6.33	5
1981	Westmoreland	USA	5.90	7
1983	Nihonkai-Chubu	Japan	7.70	2
1983	Borah Peak	USA	6.88	3
1987	Edgecumbe	NZ	6.60	23
1987	Superstition Hills	USA	6.54	8
1989	Loma Prieta	USA	6.93	61
1994	Northridge	USA	6.69	3
1995	Hyogoken-Nambu	Japan	6.90	21
1999	Kocaeli	Turkey	7.51	16
1999	Chi-Chi	Taiwan	7.62	37
2008	Achaia-Ilia	Greece	6.40	2
2010	El Mayor-Cucapah	Mexico	7.20	2
2010	Darfield	NZ	7.10	3647
2011	Christchurch	NZ	6.20	3700
2011	Tohoku	Japan	9.00	7
2012	Emilia	Italy	6.10	46
2016	Christchurch	NZ	5.70	2296
			Total	**9,908**

METHODOLOGY

Liquefaction Damage Measures (*LDMs*)

This study develops fragility-functions for three *LDMs* based on geotechnical data, wherein four CPT-based liquefaction-triggering models are used, and two *LDMs* based on readily available no-cost geospatial data. These *LDMs* are summarized at right.

Fragility Functions

The probability of liquefaction manifestation reaching or exceeding a manifestation severity, MS_i, given a computed *LDM*, is denoted $F_{MS}(LDM)$ and idealized by a lognormal distribution:

$$F_{MS}(LDM) = \Phi\left(\frac{\ln(\frac{LDM}{x_m})}{\beta}\right) \quad (1)$$

Where: Φ is the Gaussian cumulative distribution function; x_m is the distribution median, and β is the logarithmic standard deviation.

Geotechnical Models

1. Liquefaction Potential Index, *LPI* [2]
2. Modified *LPI*, termed LPI_{ISH} [3]
3. Liquefaction Severity Number, *LSN* [4]

Each is computed using the: RW98[5]; Mea06[6]; IB08[7]; and BI14[8] liq. triggering models

Geospatial Models

The geospatial models used herein were developed by Zhu et al[9] and are computed from a digital elevation model as:

$$P(X) = (1 + e^{-X})^{-1} \quad (2)$$

1. Global Geospatial Model:
$$X = 24.10 + 2.067\cdot\ln(PGA_M) + 0.355\cdot CTI - 0.4784\cdot\ln(V_{s30}) \quad (3)$$

2. Region-Specific Geospatial Model
$$X = 25.45 + 2.476\cdot\ln(PGA_M) - 0.323\cdot d_{r3} - 4.241\cdot\ln(V_{s30}) \quad (4)$$

Where: $P(X)$ = probability of surface manifestation; *CTI* = compound topographic index, PGA_M = magnitude-weighted PGA, V_{s30} = shear-wave velocity for the upper 30-m depth, estimated from topographic slope; and d_{r3} = distance to a river of Strahler-order 3 or greater.

Classifying Manifestation Severity

CES cases are classified per the Green et al[10] criteria, representative examples of which are shown in Figure 2. Global cases are classified binomially as "yes" or "no."

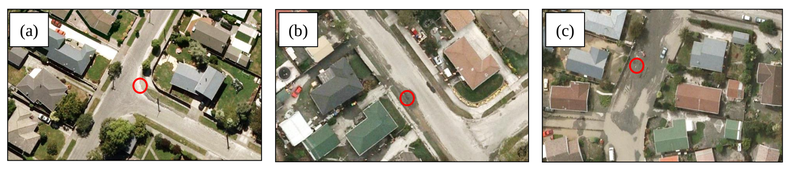

Figure 2. Representative observations of three manifestation-severity classes: (a) marginal; (b) moderate; and (c) severe

RESULTS

Fragility-functions were conditioned on: (1) *LPI*, LPI_{ISH}, and *LSN* (computed using the RW98, Mea06, IB08, and BI14 CPT-based models) for the CES and global datasets; and (2) the Zhu et al. Geospatial models for the CES dataset. As an example, the suite of functions for *LPI* / RW98 is plotted in Figure 3. A summary of all fragility-functions is provided in Tables 2 and 3.

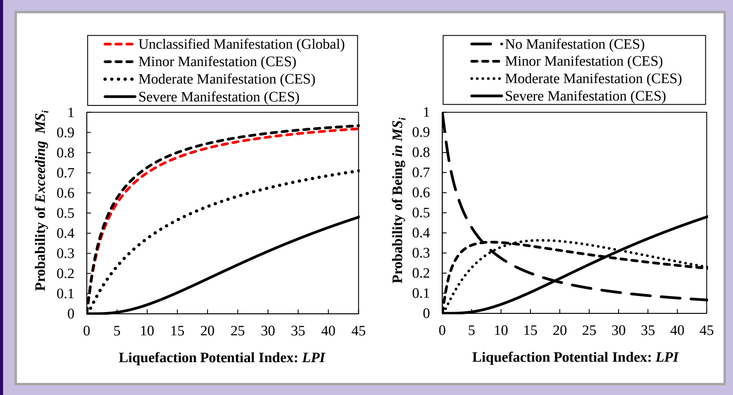

Figure 3. Probability of (a) *exceeding*; and (b) being *in* manifestation class MS_i, given *LPI* computed by RW98.

Table 2. Summary of Fragility-Functions for Geotechnical Models

Dataset	Triggering Model	Manifestation Severity	LPI x_m	LPI β	LPI Parameter Space	LPI_{ISH} x_m	LPI_{ISH} β	LPI_{ISH} Parameter Space	LSN x_m	LSN β	LSN Parameter Space
CES	RW98	Minor	3.672	1.667	LPI ≤ 50	1.766	2.249	LPI_{ISH} ≤ 43	12.836	1.747	LSN ≤ 68
		Moderate	17.420	1.722		13.955	2.349		49.495	1.584	
		Severe	47.172	0.912		86.710	1.814		202.900	1.335	
	Mea06	Minor	4.984	1.678	LPI ≤ 46	3.764	1.937	LPI_{ISH} ≤ 49	20.327	2.467	LSN ≤ 79
		Moderate	23.140	2.041		21.427	2.185		126.924	2.543	
		Severe	65.414	1.151		188.146	2.149		561.312	1.825	
	IB08	Minor	2.393	1.756	LPI ≤ 43	1.372	2.091	LPI_{ISH} ≤ 41	9.231	1.976	LSN ≤ 60
		Moderate	12.583	1.897		11.234	2.802		41.922	1.819	
		Severe	46.167	1.091		112.449	2.210		229.000	1.588	
	BI14	Minor	6.261	1.059	LPI ≤ 58	3.972	1.292	LPI_{ISH} ≤ 52	15.910	1.131	LSN ≤ 65
		Moderate	18.978	1.154		14.278	1.417		39.889	1.164	
		Severe	56.719	0.827		53.983	1.036		198.626	1.304	
Global	RW98	Unclassified Manifestation	4.061	1.726	LPI ≤ 56	0.668	3.715	LPI_{ISH} ≤ 47	8.167	1.538	LSN ≤ 67
	Mea06		4.852	1.581	LPI ≤ 52	2.242	2.299	LPI_{ISH} ≤ 42	11.551	1.456	LSN ≤ 80
	IB08		6.773	1.290	LPI ≤ 63	3.673	1.958	LPI_{ISH} ≤ 54	14.326	1.230	LSN ≤ 85
	BI14		3.101	2.280	LPI ≤ 56	1.177	3.190	LPI_{ISH} ≤ 49	8.314	1.113	LSN ≤ 61

Table 3. Summary of Fragility-Functions for Geospatial Models

Dataset	Manifestation Severity	Global Geospatial Model (Eqs. 2 and 3) x_m	Global Geospatial Model (Eqs. 2 and 3) β	Global Geospatial Model (Eqs. 2 and 3) Parameter Space	Region-Specific Geospatial Model (Eqs. 2 and 4) x_m	Region-Specific Geospatial Model (Eqs. 2 and 4) β	Region-Specific Geospatial Model (Eqs. 2 and 4) Parameter Space
CES	Minor	0.216	1.601	P(X) ≤ 0.98	0.183	0.962	P(X) ≤ 0.72
	Moderate	1.080	2.119		0.489	1.175	
	Severe	5.251	1.703		2.265	1.281	

FUTURE WORK

The functions defined by Eq. 1 and summarized in Tables 2 and 3 are preliminary and subject to further development. In this regard, several thrusts of ongoing investigation are:

1. Compile additional CES and global liquefaction case studies
2. Update PGAs for CES cases using ground-motion simulations
3. Account for aleatoric and epistemic uncertainties
4. Apply geospatial models to global case studies
5. Determine whether CES results are applicable worldwide
6. Assess whether the lognormal distribution is appropriate

REFERENCES

[1] Maurer, B.W., Green, R.A., Cubrinovski, M., and Bradley, B. (2015). "Assessment of CPT-based methods for liquefaction evaluation in a liquefaction potential index framework." *Géotechnique* 65(5): 328-336.

[2] Iwasaki, T., Tatsuoka, F., Tokida, K., & Yasuda, S. (1978). "A practical method for assessing soil liquefaction potential based on case studies at various sites in Japan." *2nd Intl Conference on Microzonation,* Nov 26-Dec 1, San Francisco, USA.

[3] Maurer, B.W., Green, R.A., and Taylor, O.S. (2015). "Moving towards an improved index for assessing liquefaction hazard: lessons from historical data." *Soils and Foundations* 55(4): 778-787.

[4] Van Ballegooy, S., Malan, P., Lacrosse, V., Jacka, M.E., Cubrinovski, M., Bray, J.D., O'Rourke, T.D., Crawford, S.A., and Cowan, H. (2014). "Assessment of liquefaction-induced land damage for residential Christchurch." *Earthquake Spectra*, 30(1): 31-55.

[5] Robertson, P.K. and Wride, C.E. (1998). "Evaluating cyclic liquefaction potential using cone penetration test." *Canadian Geotechnical Journal*, 35(3): 442-459.

[6] Moss, R.E.S, Seed, R.B., Kayen, R.E., Stewart, J.P., Der Kiureghian, A., & Cetin, K.O. (2006). "CPT-based probabilistic and deterministic assessment of in situ seismic soil liquefaction potential." *J. Geotechnical and Geoenvironmental Engineering,* 132(8): 1032-1051.

[7] Idriss, I.M. & Boulanger, R.W. (2008). "Soil liquefaction during earthquakes." Monograph MNO-12, Earthquake Engineering Research Institute, Oakland, CA, 261 pp.

[8] Boulanger, R.W. and Idriss, I.M. (2014). "CPT and SPT based liquefaction triggering procedures." *Report No. UCD/CGM.-14/01*, UC Davis, CA, USA.

[9] Zhu, J., Daley, D., Baise, L.G., Thompson, E.M., Wald, D.J., and Knudsen, K.L. (2014). "A geospatial liquefaction model for rapid response and loss estimation." *Earthquake Spectra* 31(3): 1813-1837.

[10] Green, R.A., Cubrinovski, M., Cox, B., Wood, C., Wotherspoon, L., Bradley, B., & Maurer, B.W. (2014). "Select Liquefaction Case Histories from the 2010-2011 Canterbury Earthquake Sequence." *Earthquake Spectra*, 30(1): 131-153.